

The presynaptic scaffolding protein Piccolo organizes the readily releasable pool at the calyx of Held

Daniel Parthier^{1,2} , Thomas Kuner¹ and Christoph Körber¹ 

¹Institute of Anatomy and Cell Biology, Department of Functional Neuroanatomy, Heidelberg University, Heidelberg, Germany

²Present address: Neuroscience Research Center, Charité Universitätsmedizin, Berlin, Germany

Edited by: Ole Paulsen & Maike Glitsch

Key points

- Bassoon and Piccolo do not mediate basal synaptic vesicle release at a high-frequency synapse.
- Knockdown of Bassoon increases short-term depression at the calyx of Held.
- Both Bassoon and Piccolo have shared functions in synaptic vesicle replenishment during high-frequency synaptic transmission.
- Piccolo organizes the readily releasable pool of synaptic vesicles. It safeguards a fraction of them to be not immediately available for action potential-induced release. This enables the synapse to sustain high-frequency synaptic transmission over long periods.

Abstract Synaptic vesicles (SVs) are released at the active zone (AZ), a specialized region of the presynaptic plasma membrane organized by a highly interconnected network of multidomain proteins called the cytomatrix of the active zone (CAZ). Two core components of the CAZ are the large, highly homologous scaffolding proteins Bassoon and Piccolo, whose function is not well understood. To investigate their role in synaptic transmission, we established the small hairpin RNA (shRNA)-mediated *in vivo* knockdown (KD) of Bassoon and Piccolo at the rat calyx of Held synapse. KD of Bassoon and Piccolo, separately or simultaneously, did not affect basic SV release. However, short-term depression (STD) was prominently increased by the KD of Bassoon, whereas KD of Piccolo only had a minor effect. The observed alterations in STD were readily explained by reduced SV replenishment in synapses deficient in either of the proteins. Thus, the regulation of SV refilling during ongoing synaptic activity is a shared function of Bassoon and Piccolo, although Bassoon appears to be more efficient. Moreover, we observed the recruitment of slowly-releasing SVs of the readily-releasable pool (RRP), which are normally not available for action potential-induced release, during high-frequency stimulation in Piccolo-deficient calyces. Therefore, the results obtained in the present study suggest a novel and specific role for Piccolo in the organization of the subpools of the RRP.

(Received 6 July 2017; accepted after revision 28 November 2017; first published online 30 November 2017)

Corresponding author C. Körber: Institute of Anatomy and Cell Biology, Department of Functional Neuroanatomy, Heidelberg University, Im Neuenheimer Feld 307, 69120 Heidelberg, Germany. Email: koerber@ana.uni-heidelberg.de

Introduction

Information transfer between neurons relies on the precisely timed fusion of synaptic vesicles (SVs) at the active zone (AZ), a specialized region at the presynaptic plasma membrane. The AZ is organized by the cytomatrix of the active zone (CAZ), a dense mesh-

work of multidomain proteins, including Munc13s, Rab3-interacting molecules (RIMs), RIM-binding proteins (RIM-BPs), ELKS/CAST, Liprins- α and the large and highly homologous scaffolding proteins Bassoon and Piccolo (Südhof, 2012; Gundelfinger & Fejtova, 2012). The CAZ provides, amongst other functions, a structural framework for the precise positioning of voltage-gated

calcium channels (VGCCs) and SVs relative to each other to match the physiological requirements of the synapse. Recent studies assigned functional roles to many of the CAZ proteins (Südhof, 2012; Rizzoli, 2014; Körber & Kuner, 2016), but the roles of Bassoon and Piccolo remained enigmatic.

Since Bassoon and Piccolo are highly homologous, they share a large number of interaction partners, including other scaffolding proteins, the SV docking protein Munc13 and components of the ubiquitin-proteasome. However, there are also interactions unique to either of the proteins. Piccolo, for example, is linked to the regulation of the actin cytoskeleton (Gundelfinger *et al.* 2016). Knockout (KO) of Bassoon has been shown to retard the SV replenishment at the AZ, particularly at high-frequency synapses such as the cerebellar mossy fibre to granule cell synapse and the endbulb of Held in the auditory brainstem (Hallermann *et al.* 2010; Mendoza Schulz *et al.* 2014). Moreover, Bassoon is involved in the localization of VGCCs at the AZs of both ribbon synapses, where it also assists in ribbon anchoring (Khimich *et al.* 2005; Frank *et al.* 2010; Jing *et al.* 2013), and bouton type synapses (Davydova *et al.* 2014). Piccolo has received much less attention and its function remained controversial. Piccolo-KD in hippocampal cultured neurons resulted in increased SV mobility, enhanced SV exocytosis and reduced actin polymerization (Leal-Ortiz *et al.* 2008; Waites *et al.* 2011), whereas the same type of neurons obtained from KO mice failed to show alterations in SV release, even when Bassoon was knocked down simultaneously (Mukherjee *et al.* 2010).

Besides these functions, related to SV release and AZ organization, Bassoon and Piccolo have also been implicated in CtBP1-mediated, activity-dependent gene regulation via synapse-to-nucleus signalling (Ivanova *et al.* 2015) and maintenance of AZ integrity by inhibition of the ubiquitin-proteasome (Waites *et al.* 2013) and autophagy (Okerlund *et al.* 2017).

In the present study, we aimed to examine the roles of Bassoon and Piccolo in synaptic transmission at the calyx of Held, a giant axosomatic synapse in the medial nucleus of the trapezoid body (MNTB) of the auditory brainstem that has evolved as a prime model for presynaptic mechanisms (Borst & Soria van Hoeve, 2012). Therefore, we established small hairpin RNA (shRNA)-mediated *in vivo* KDs of Bassoon and Piccolo, separately and simultaneously, in the globular bushy cells of the contralateral ventral cochlear nucleus (VCN), which give rise to the calyces of Held. We observed alterations in SV replenishment at the AZ during ongoing synaptic activity in calyces that were deficient of Bassoon or Piccolo. Although the effect was more pronounced in Bassoon-KD calyces, the regulation of SV replenishment is a common role of both proteins. Moreover, we observed a unique function of Piccolo that was not shared with Bassoon:

at Piccolo-deficient calyces, slowly-releasing SVs were amenable during trains of action potentials (APs), which became evident by the appearance of a second kinetic component during recovery from STD that is absent in wild type or Bassoon-deficient calyces. Thus, we were able to assign distinct and overlapping functions to these two major CAZ proteins.

Methods

Ethical approval

All experiments were conducted in accordance with the German animal welfare guidelines and approved by the Regierungspräsidium Karlsruhe. The reported experiments complied with the ethical principles and checklist of *The Journal of Physiology* (Grundy, 2015). Sprague-Dawley dams (Charles River Laboratories, Sulzfeld, Germany) were kept in individually ventilated cages and given *ad libitum* access to food and water. Additional nesting material was provided. Pregnant rats arrived in the animal facility 1 week prior to delivery. Pups that had undergone stereotaxic surgery were returned to their mothers and stayed with them until the day of the experiments.

AAV constructs

Previously published sequences coding for shRNAs directed against Bassoon or Piccolo mRNAs or a scrambled control (Leal-Ortiz *et al.* 2008; Waites *et al.* 2011) were subcloned into an adeno-associated virus (AAV) vector in which shRNA expression was driven via the U6 (Bassoon and scrambled) or H1 (Piccolo) promoter. The double-KD was achieved by expression of both shRNAs from the same viral vector, each driven by their respective promoter. All shRNA-expressing vectors additionally coded for the fluorescent reporter mOrange2 under the CAG promoter in cis (Körber *et al.* 2015). Chimeric AAV particles of the serotypes 1 and 2 were prepared as described previously (Körber *et al.* 2015; Schwenger & Kuner, 2010).

Stereotaxic injection

Anaesthetized two days old Sprague-Dawley rats of either sex were injected with AAV particles into the VCN as described previously (Dondzillo *et al.* 2010; Schwenger & Kuner, 2010; Wimmer *et al.* 2004). In brief, rats were deeply anaesthetized using isoflurane and then aligned in the stereotax (Kopf Instruments, Tujunga, CA, USA). A craniectomy of ~2 mm in diameter was performed and ~2.5 μ L of virus solution was evenly distributed to co-ordinates relative to bregma and midline (x, y, mm): 0.7, -6.6; 0.7, -7.0; 0.7, -7.4; 0.9, -6.8, 0.9, -7.2; 0.9, -7.6 using a custom build manipulator (Wimmer *et al.*

2004). Z- and A-positions were kept constant at 0.45 and 6.5 mm, respectively. The rats recovered within minutes and were returned to their mothers.

Immunohistochemistry

Rats previously injected with AAV particles were deeply anaesthetized (Narcoren; Merial GmbH, Hallbergmoos, Germany; 500 mg kg⁻¹ bodyweight i.p.) at postnatal day 12/13 and transcardially perfused with PBS followed by 4% paraformaldehyde (PFA) dissolved in PBS. Brains were removed and post-fixed for 2–3 h in 4% PFA at 4°C. PFA was removed by three washes in PBS before the brainstem was cut into slices (thickness 100 μm) using a vibratome (Sigmund Elektronik GmbH, Hüllfhardt, Germany).

Antibody staining was performed as described extensively by Schwenger and Kuner (2010). Primary antibodies against Bassoon (dilution 1:1000; catalogue number ADI-VAM-PS003, Enzo Life Science, Farmingdale, NY, USA) and Piccolo (dilution 1:250; catalogue number 142 104; Synaptic Systems, Göttingen, Germany) were used. Appropriate Alexa dye coupled secondary antibodies (Invitrogen, Carlsbad, CA, USA) were used at dilutions of 1:1000.

Stained brainstem sections were examined by confocal microscopy. Image stacks were acquired using a TCS SP5 microscope (Leica Microsystems, Wetzlar, Germany) equipped with a 63× HCX PL APO (1.45 NA) objective. 3-D reconstruction of whole calyces and quantitative image analyses of fluorescence signals was performed using Amira, version 5.0 (Thermo Fisher Scientific Inc., Waltham, MA, USA) as described previously (Dondzillo *et al.* 2010; Körber *et al.* 2015). Briefly, the membrane-bound green fluorescent protein (mGFP) fluorescence signal was thresholded and 3-D segmented to reconstruct the calyx of interest. The immunoreactive signal within these calyces was thresholded and quantitatively analysed using Amira software (version 5.0).

Electrophysiology

To maintain brain integrity for the electrophysiological recordings, rats previously injected with AAVs were killed by decapitation at postnatal day 12/13 in compliance with Annex IV of European Directive 2010/63/EU. Brains were removed into ice-cold slicing solution containing (in mM): 125 NaCl, 25 NaHCO₃, 2.5 KCl, 1.25 NaH₂PO₄, 3 myo-inositol, 2 Na-pyruvate, 0.4 ascorbic acid, 0.1 CaCl₂, 3 MgCl₂ and 25 glucose aerated with carbogen (5% CO₂ in O₂). Brainstem slices (thickness 300 μm) were prepared on a vibratome (VT1200S; Leica) and stored in artificial cerebrospinal fluid (aCSF) (in mM: 125 NaCl, 25 NaHCO₃, 2.5 KCl, 1.25 NaH₂PO₄, 2 CaCl₂, 1 MgCl₂ and 25 glucose aerated with carbogen, pH 7.3) at 37°C for 45 min and at room temperature (21 ± 1°C) thereafter.

Whole-cell patch clamp recordings were established from MNTB principal neurons, targeted by either a wild-type (WT) calyx or a calyx expressing one of the shRNAs, using an EPC-10/2 amplifier controlled by Patchmaster software (HEKA, Lambrecht, Germany). shRNA-expressing calyces were identified by mOrange2 expression. All experiments were performed at room temperature. Voltage clamp recordings were performed in aCSF at a holding potential of -70 mV using pipettes filled with pipette solution containing (in mM): 130 Cs gluconate, 10 CsCl, 10 Hepes, 10 TEA-Cl, 5 Na₂-phosphocreatine, 5 EGTA, 4 Mg-ATP and 0.3 GTP (pH 7.2). Pipettes had open tip resistances smaller than 2.7 MΩ. Series resistances ranged from 3 to 6 MΩ and were compensated for by >90%. In some experiments, aCSF was supplemented with 1 mM kynurenic acid (Kyn) and 0.1 mM cyclothiazide (CTZ) to block AMPA receptor saturation and desensitization, respectively. Kyn and CTZ were purchased from Abcam (Cambridge, UK). During experiments with a reduced extracellular calcium concentration, calcium was replaced by magnesium to keep the concentration of divalent cations constant. The afferent fibres of the calyx of Held were stimulated via a parallel bipolar electrode (FHC Inc., Bowdoin, ME, USA) placed close to midline (2–6 V stimuli, 100 μs in duration). Currents were digitized at sampling rates of 10–100 kHz and Bessel-filtered at 2.9 kHz.

Statistical analysis

Data were analysed using custom-written IGOR routines (Wavemetrics, Lake Oswego, OR, USA) and Prism (version 5.0, GraphPad software, La Jolla, CA, USA). Statistical significance was determined by one-way ANOVA followed by Dunnett's test or two-tailed, unpaired *t* test (**P* < 0.05, ***P* < 0.01, ****P* < 0.001), except for recovery from depression experiments where a Kruskal–Wallis test (non-parametric ANOVA) followed by Dunn's test (**P* < 0.05) was used. The WT group was used as a reference in *post hoc* tests. Data are presented as the mean ± SEM.

Results

KD of Bassoon and Piccolo at the calyx of Held

To investigate the functional roles of Bassoon and Piccolo in synaptic transmission, we established a shRNA-mediated *in vivo* KD of both proteins. We took advantage of previously published shRNA sequences specific for either Bassoon or Piccolo, as well as a scrambled (SC) control shRNA (Leal-Ortiz *et al.* 2008; Waites *et al.* 2011). These sequences were used to generate AAVs containing either one of the two KD-shRNA sequences

or the control SC-shRNA. Additionally, we produced AAVs containing both KD-shRNAs on the same viral vector construct under separate promoters (see Methods). All AAVs expressed the fluorescent reporter mOrange2 in cis allowing the identification of shRNA-expressing calyces. AAV particles containing the sequences of either of the shRNAs were injected into the VCN of P2 rats. Additionally, we co-injected AAVs expressing mGFP to delineate the plasma membrane of individual calyces. KD efficiency in individual synapses was examined after 10 days of *in vivo* incubation by immunohistochemistry. Calyces expressing either of the shRNAs, identified by mOrange2-fluorescence, or WT control calyces were 3-D-reconstructed from confocal image stacks using the mGFP-signal (Dondzillo *et al.* 2010; Körber *et al.* 2015) and the expression levels of Bassoon and Piccolo at the single calyx were determined. We found strong and specific reductions of Bassoon and Piccolo immunosignals in calyces expressing the respective shRNAs compared to WT and SC-shRNA controls (Fig. 1). Bassoon expression levels were reduced by ~80 % compared to WT in double knockdown (DKD) and Bsn-KD calyces (fraction of

calyx volume occupied by Bassoon immunofluorescence signal: WT: $8.70 \pm 1.54\%$, DKD: $1.74 \pm 0.74\%$, Bsn-KD: $0.99 \pm 0.19\%$, $P < 0.0001$, one-way ANOVA, $n = 7-10$ calyces), whereas the expression of the SC-shRNA or the shRNA directed against Piccolo (Pcl-KD) had no effects on Bassoon expression (SC: $5.96 \pm 1.01\%$, Pcl-KD: $8.71 \pm 1.73\%$, $n = 7-10$) (Fig. 1B). Similarly, Piccolo expression was reduced by ~90% in Pcl-KD and DKD calyces (fraction of calyx volume occupied by Piccolo immunofluorescence signal: WT: $6.83 \pm 1.97\%$, DKD: $0.40 \pm 0.14\%$, Pcl-KD: $0.39 \pm 0.07\%$, $n = 7-15$ calyces, $P < 0.0001$, one-way ANOVA) but not in calyces expressing SC- or Bsn-KD-shRNA (SC: $6.48 \pm 0.75\%$, Bsn-KD: $7.19 \pm 1.19\%$) (Fig. 1A and C). Since recent studies reported the loss of AZ components in DKD synapses (Waites *et al.* 2013; Okerlund *et al.* 2017), we examined the amount of synaptophysin in DKD calyces but did not observe any obvious difference compared to SC-shRNA and WT controls (data not shown). Thus, shRNA-mediated KD of Bassoon and Piccolo at the calyx *in vivo* is efficient and specific without inducing the loss of AZs.

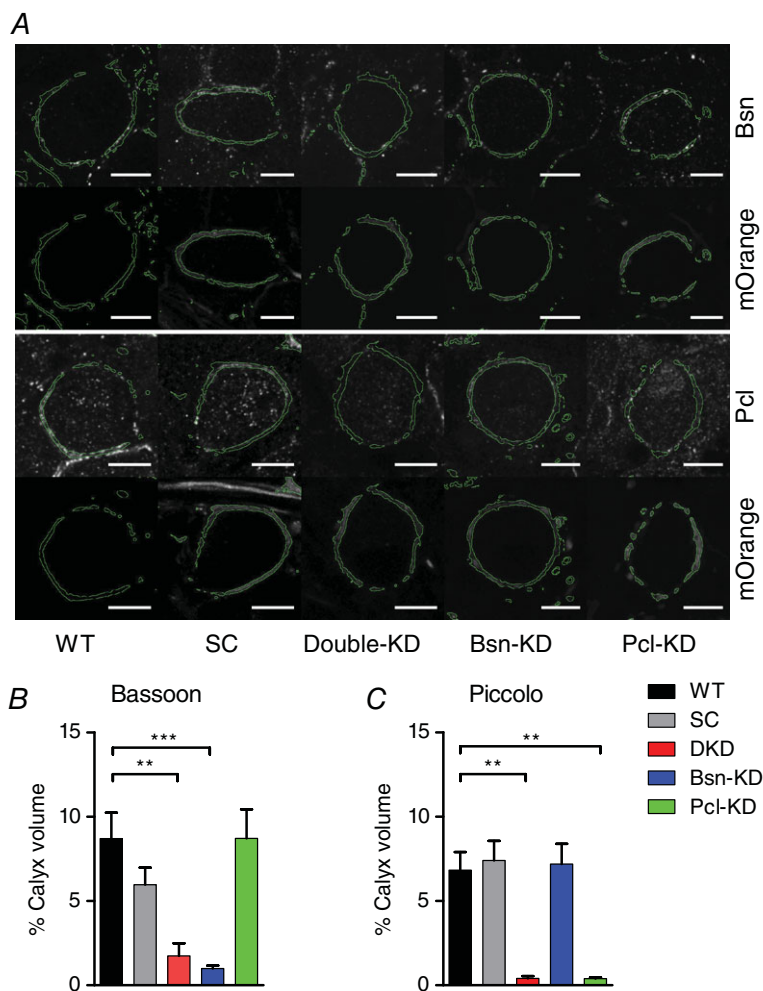


Figure 1. Bassoon and Piccolo are efficiently and specifically knocked down at the calyx of Held *in vivo*

A, representative confocal sections of individual calyces delineated by mGFP (green outline) and immunostained for Bassoon (top) and Piccolo (bottom). Calyces expressing a shRNA were identified by mOrange2 fluorescence (shown below the immunosignal). Scale bar: 10 μm . [Correction made on 23 January 2018 after first online publication: Scale bar measurement was added.] B and C, quantification of Bassoon and Piccolo immunosignal in identified calyces ($n = 7-15$ calyces). Error bars represent the SEM.

SV release is independent of Bassoon and Piccolo the calyx of Held

SVs can be released in three different modes: synchronously (immediately after an AP) asynchronously (delayed after an AP) and spontaneously (in the absence of an AP) (Kaesler & Regehr, 2014). We first examined whether Bassoon and Piccolo play a role in any of the three release modes. Therefore, we recorded spontaneous

EPSCs from MNTB principal neurons in acute brainstem slices prepared from postnatal day 12/13 rats. MNTB neurons that were targeted by shRNA-expressing calyces were identified by mOrange2 fluorescence. Spontaneous release was not changed by KD of Bassoon or Piccolo (Fig. 2A and B). Neither frequency, nor amplitude or the kinetics of spontaneous release events were altered by the expression of any of the shRNAs compared to WT control synapses (Fig. 2B and Table 1), suggesting that the basic

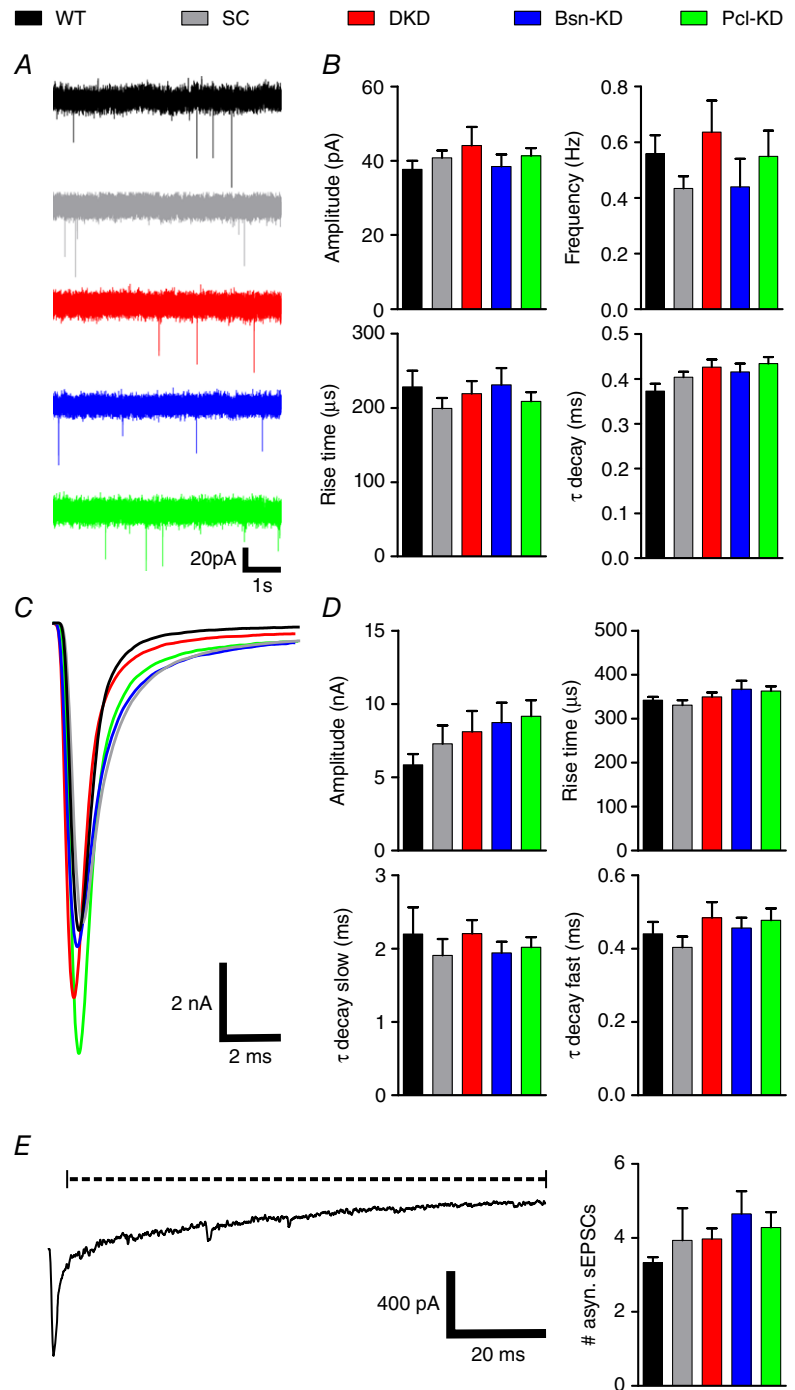


Figure 2. Bassoon and Piccolo KD do not affect basal SV release
 A, representative current traces of spontaneous EPSCs. B, quantification of spontaneous EPSC amplitude, frequency and kinetic properties. C, superimposed representative current traces of evoked EPSCs. D, quantification of evoked EPSC amplitude and kinetic properties. E, representative current trace recorded after a train of 50 APs delivered at 100 Hz to induce asynchronous release, which is determined by the number of miniature EPSCs in the time window indicated by the dashed line (left) and quantification of miniature EPSC counts (right) ($n = 9-11$). Error bars represent the SEM. [Correction made on 23 January 2018 after online publication: Scale bar in Fig. 2E was corrected from 200 ms to 20 ms.]

Table 1. Comparison of basal synaptic release parameters between WT calyces and calyces expressing different shRNAs

Parameter	WT	SC	DKD	Bsn-KD	Pcl-KD	Statistical test
sEPSC						
<i>n</i>	6	9	7	8	9	
Amplitude (pA)	37.70 ± 2.29	40.53 ± 2.13	44.55 ± 4.23	38.47 ± 3.20	41.36 ± 2.03	One-way ANOVA NS
Rise time (μs)	228.5 ± 21.6	199.5 ± 14.0	219.5 ± 17.0	231.3 ± 22.7	208.9 ± 12.6	One-way ANOVA NS
τ _{decay} (ms)	0.3727 ± 0.0170	0.4042 ± 0.0118	0.4267 ± 0.0170	0.4156 ± 0.0187	0.4346 ± 0.0143	One-way ANOVA NS
Frequency (Hz)	0.56 ± 0.07	0.43 ± 0.04	0.64 ± 0.11	0.44 ± 0.10	0.55 ± 0.09	One-way ANOVA NS
eEPSC						
<i>n</i>	12	11	10-11	9-11	9-10	
Amplitude (nA)	5.856 ± 0.734	7.289 ± 1.251	8.116 ± 1.404	8.730 ± 1.360	9.167 ± 1.099	One-way ANOVA NS
Rise time (μs)	342.2 ± 7.5	330.8 ± 11.2	349.3 ± 10.4	366.9 ± 19.2	362.9 ± 10.8	One-way ANOVA NS
τ _{decay} fast (ms)	0.4403 ± 0.0325	0.4036 ± 0.2929	0.4842 ± 0.0425	0.4562 ± 0.0281	0.4775 ± 0.0325	One-way ANOVA NS
τ _{decay} slow (ms)	2.200 ± 0.363	1.907 ± 0.225	2.205 ± 0.183	1.943 ± 0.152	2.019 ± 0.138	One-way ANOVA NS
asynchronous EPSCs						
<i>n</i>	12	11	11	9	9	
#/100 ms post stimulus	3.39 ± 0.15	4.08 ± 0.94	4.09 ± 0.28	4.67 ± 0.68	4.22 ± 0.41	One-way ANOVA NS
Kyn/CTZ						
<i>n</i>	7				5	
Amplitude EPSC (nA)	3.447 ± 0.739				2.600 ± 0.384	t test NS

NS, not significant.

release machinery works independently of Bassoon and Piccolo. Next, we examined synchronous release in calyces deficient in Bassoon and/or Piccolo by recording single EPSCs evoked by low frequency stimulation (0.1 Hz). Although the EPSC amplitudes were highly variable, ranging from 3 to 15 nA in all groups, we did not detect any significant changes in EPSC amplitude or kinetic upon the KD of Bassoon and/or Piccolo compared to WT or SC-shRNA controls (Fig. 2C and D and Table 1). However, AMPA receptor saturation or desensitization could have compromised our results, thereby obscuring a possible role of Piccolo or Bassoon in evoked, synchronous SV release. To exclude this possibility, we recorded single EPSCs evoked at 0.1 Hz from WT and Pcl-KD calyces in the presence of 1 mM Kyn and 0.1 mM CTZ to block AMPA receptor saturation and desensitization, respectively. Pcl-KD synapses were chosen because they showed the largest EPSC amplitudes in normal aCSF and were thus most prone to be compromised by AMPA receptor saturation and desensitization. We did not observe any significant difference in EPSC amplitude between WT and Pcl-KD calyces in the presence of Kyn and CTZ (Table 1), thereby confirming the results obtained in normal aCSF. Finally, we investigated asynchronous release, which can be observed as a transient increase in the number of miniature EPSCs after a train of high-frequency stimuli (50 APs at 100 Hz) at the calyx. Quantification of miniature EPSCs in the 100 ms after the cessation of the stimulus train showed no change in asynchronous release in calyces deficient in Bassoon and/or Piccolo compared to controls (Fig. 2E and F and Table 1). We thus conclude that basal SV release is independent of Bassoon and Piccolo at the calyx of Held.

STD is regulated by Bassoon and Piccolo

STD, the decay of EPSC amplitudes during trains of high-frequency stimulation, is a prominent feature of the calyx of Held (Borst & Soria van Hoeve, 2012) and has been shown to be regulated by Bassoon at the cerebellar mossy fibre to granule cell synapse and the endbulb of Held (Hallermann *et al.* 2010; Mendoza Schulz *et al.* 2014). We investigated STD in response to AP-trains applied at 100 Hz (50 stimuli). In calyces expressing either Bsn-KD- or DKD-shRNA, we detected a decrease in the time constant of the mono-exponential function used to describe the EPSC amplitude decay and thus an acceleration of STD (Fig. 3A–C and Table 2). STD was only significantly accelerated in Bassoon-deficient calyces, whereas the expression of SC-shRNA or the KD of Piccolo alone did not lead to significant changes in the time constant of EPSC amplitude decay compared to WT calyces (Table 2). To exclude the possibility that AMPA receptor saturation or desensitization obscures effects of Pcl-KD on the time course of STD, we

investigated STD of WT and Pcl-KD calyces in response to 100 Hz AP-trains in aCSF containing 1 mM Kyn and 0.1 mM CTZ (Table 2). We did not observe any difference in the time course of EPSC amplitude decay between WT and Pcl-KD calyces, thereby confirming the results obtained in normal aCSF. Of note, the actual time constants of EPSC amplitude decay are slower in aCSF containing Kyn and CTZ because CTZ slows AMPA receptor kinetics (Traynelis *et al.* 2010). In addition to the acceleration in STD time course, we observed a reduction in the paired-pulse ratio (PPR) between the first and the second EPSC in the train in synapses with reduced Bassoon expression, whereas a reduction in Piccolo expression did not result in significantly altered PPR (Fig. 3D and Table 2). Besides these two STD parameters that were dependent on Bassoon, we found that the relative extent of depression was larger in calyces expressing any of the KD-shRNAs, resulting in a more complete STD (Fig. 3E and Table 2). Interestingly, the steady-state EPSC amplitude was reduced in calyces expressing either Bsn-KD or DKD shRNAs, although this reduction did not reach significance (Table 2). These results suggest that Bassoon and Piccolo have partially overlapping functions in the regulation of STD. However, the regulatory effect of Piccolo appears to be minor in comparison to Bassoon since Bassoon-deficient calyces showed alterations in all three STD parameters, whereas Piccolo selectively affected the amount of depression.

The effect of Bassoon on STD is independent of vesicular release probability

Short-term plasticity (STP) is dependent on the vesicular release probability (P_r) of the synapse (Zucker & Regehr, 2002). We therefore examined whether the effect of Bassoon deficiency on STP was dependent on P_r . Therefore, we investigated STP in response to AP-trains (100 Hz, 50 stimuli) in WT and Bsn-KD calyces using aCSF that contained only 1.5 mM calcium. Reducing the extracellular calcium concentration leads to less calcium influx during AP-trains and therefore a reduced P_r . Synapses with a low initial P_r show short-term facilitation (STF) instead of STD (Zucker & Regehr, 2002). In WT synapses, deliverance of AP-trains lead to a brief episode (two or three stimuli) of initial STF followed by STD (Fig. 4A), instead of the immediate STD observed in normal aCSF, confirming the reduced P_r . Applying the same stimulation to Bsn-KD calyces did not result in an initial STF followed by STD but, instead, in an immediate STD albeit with a higher PPR and a slower time course than in normal aCSF (Fig. 4). Comparison of STP parameters between WT and Bsn-KD calyces confirmed that the effects of Bsn-KD described in normal aCSF were independent of the vesicular P_r because they persisted

in aCSF containing reduced extracellular calcium (Fig. 4 and Table 2).

Bassoon and Piccolo determine SV replenishment at the AZ

The regulation of STD by Bassoon has been shown to be a result of Bassoon speeding-up SV replenishment, comprising the delivery of SV to the AZ under ongoing synaptic activity, thereby ensuring the availability of SVs for release during periods of high presynaptic activity and thus limiting STD (Hallermann *et al.* 2010; Mendoza Schulz *et al.* 2014). We determined the replenishment rate of SVs at the AZ and the RRP size using the cumulative EPSC analysis of 100 Hz AP-trains. In this analysis, the cumulative EPSC amplitude is plotted against the stimulus number. Late during the stimulus train, EPSCs are largely carried by SVs that are newly replenished to the AZ, leading to steady-state release and thus a linear plot (Fig. 5A). A line fit through the linear, steady-state part of the graph yields two parameters: the slope, which is a measure of the rate of SV replenishment at the AZ, and the back-extrapolated intercept of the fit with the y -axis, which determines the

RRP size (Schneggenburger *et al.* 1999) (Fig. 5). The replenishment rate was normalized to the initial EPSC amplitude by dividing the slope of the line fit by the EPSC amplitude, thereby taking inter-synapse variability into account (Fig. 5C). We did not observe significant changes in the size of the RRP in synapses expressing either of the shRNAs (Fig. 5B). However, it has been suggested that, in some cases, the method of Elmqvist and Quastel yields more reliable RRP size estimates (Neher, 2015) than the back-extrapolating fit used here. In this alternative analysis, the EPSC amplitude is plotted against the cumulative EPSC and the intersection with the x -axis of a line fit through the initial, linear part of the plot gives a RRP size measure (Elmqvist & Quastel, 1965, Taschenberger *et al.* 2002, Butola *et al.* 2017). Using this analysis, we again did not observe significant differences in RRP size in calyces expressing either of the shRNAs (Fig. 5D and E and Table 2). In contrast to RRP size, we found a pronounced slowing of SV replenishment, as indicated by the reduction in normalized replenishment rate (i.e. slope of the line fit/initial EPSC amplitude), in calyces with reduced Bassoon or Piccolo expression compared to WT and SC-shRNA controls (Fig. 5A

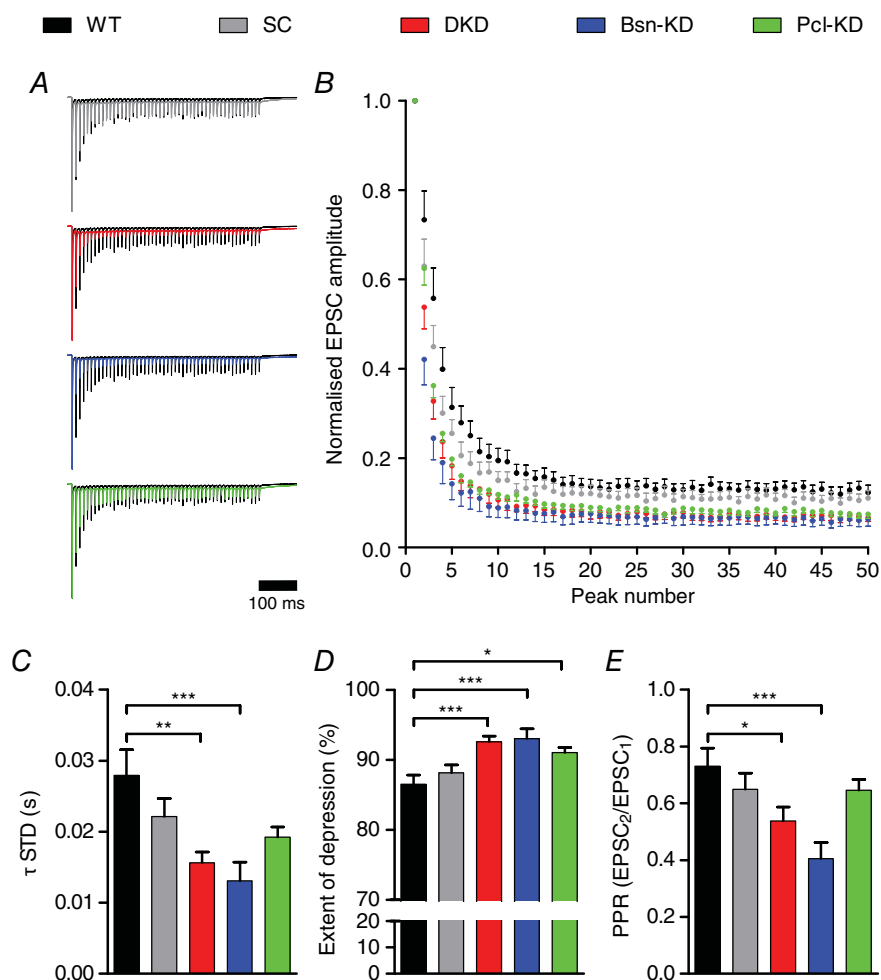


Table 2. Comparison of STP and recovery parameters between WT calyces and calyces expressing different shRNAs

Parameter	WT	SC	DKD	Bsn-KD	Pcl-KD	Statistical test	Post hoc test
STD (10 Hz)							
<i>n</i>	12	11	11	10	10		
τ (s)	0.0279 ± 0.004	0.0221 ± 0.003	0.0156 ± 0.002	0.0131 ± 0.003	0.0192 ± 0.001	One-way ANOVA, <i>P</i> = 0.0014	Dunnett's test, WT vs. DKD, <i>P</i> < 0.01; WT vs. Bsn-KD <i>P</i> < 0.001
Depression (%)	86.5 ± 1.3	88.2 ± 1.1	92.6 ± 0.8	93.1 ± 1.4	91.1 ± 0.7	One-way ANOVA, <i>P</i> = 0.0003	Dunnett's test, WT vs. DKD, <i>P</i> < 0.001; WT vs. Bsn-KD, <i>P</i> < 0.001; WT vs. Pcl-KD, <i>P</i> < 0.05
PPR	0.73 ± 0.06	0.65 ± 0.06	0.54 ± 0.05	0.40 ± 0.06	0.65 ± 0.04	one-way ANOVA, <i>P</i> = 0.002	Dunnett's test, WT vs. Bsn-KD, <i>P</i> < 0.001
Steady-state EPSC (pA)	701 ± 86	703 ± 86	513 ± 70	525 ± 93	675 ± 75		one-way ANOVA NS
STD (100 Hz) Kyn/CTZ							
<i>n</i>	7				5		
τ_{STD} (s)	0.7298 ± 0.0249				0.7499 ± 0.0201	t test NS	
STD (100 Hz) 1.5 mM [Ca ²⁺] _e							
<i>n</i>	9			6			
τ (s)	0.0675 ± 0.011			0.0289 ± 0.005		t test, <i>P</i> = 0.016	
Depression (%)	68.9 ± 5.6			88.2 ± 2.6		t test, <i>P</i> = 0.02	
PPR	1.27 ± 0.11			0.87 ± 0.1		t test, <i>P</i> = 0.025	
RRP							
<i>n</i>	12	11	11	10	10		
RRP size (nA)	18.32 ± 2.30	16.89 ± 1.31	18.20 ± 2.13	19.17 ± 2.73	24.84 ± 3.42	One-way ANOVA, NS	
Normal replenishment rate (ms ⁻¹)	0.014 ± 0.001	0.012 ± 0.002	0.008 ± 0.001	0.008 ± 0.001	0.009 ± 0.001	One-way ANOVA, <i>P</i> = 0.0013	Dunnett's test, WT vs. DKD, <i>P</i> < 0.01; WT vs. Bsn-KD, <i>P</i> < 0.01; WT vs. Pcl-KD, <i>P</i> < 0.05
RRP size Elmquist and Quastel (nA)	24.63 ± 3.69	21.17 ± 1.67	19.59 ± 2.13	20.84 ± 2.81	28.48 ± 3.56	one-way ANOVA NS	
Recovery from STD							
<i>n</i>	8	6	6	8	7		
τ_{fast} (s)	2.59 ± 0.98	2.54 ± 0.90	0.11 ± 0.05	2.37 ± 0.90	0.10 ± 0.01	Kruskal–Wallis test, <i>P</i> = 0.0034	Dunn's test, WT vs. DKD, <i>P</i> < 0.05; WT vs. Pcl-KD, <i>P</i> < 0.05;
Amplitude τ_{fast} (%)	0.30 ± 0.03	0.34 ± 0.07	0.14 ± 0.02	0.34 ± 0.07	0.20 ± 0.02	Kruskal–Wallis test, <i>P</i> = 0.0221	Dunn's test, WT vs. DKD, <i>P</i> < 0.05
τ_{slow} (s)	6.83 ± 1.22	6.17 ± 1.63	9.16 ± 1.68	6.48 ± 1.16	3.93 ± 0.41	Kruskal–Wallis test NS	
Amplitude τ_{slow} (%)	0.52 ± 0.08	0.57 ± 0.07	0.82 ± 0.06	0.65 ± 0.13	0.70 ± 0.03	Kruskal–Wallis test NS	

NS, not significant.

and C and Table 2). We therefore conclude that the increased extent of depression in calyces expressing either of the shRNAs is caused by a slowing of SV replenishment at the AZ. This is further supported by a reduction in steady-state EPSC amplitude (albeit non-significant) observed late in the stimulus train in calyces expressing Bsn-KD- and DKD-shRNAs. Of note, we did not observe this reduction in synapses expressing Pcl-KD-shRNA, although SV replenishment was also slowed at these synapses (Table 2). These findings suggest that both proteins regulate the SV replenishment rate, which in turn affects STD.

Piccolo organizes the RRP

At the calyx of Held, the RRP can be further divided into two subpools of roughly equal size: one containing fast-releasing SVs that are slowly refilled and the other consisting of SVs that are slowly released but quickly recovered (Wu & Borst, 1999; Sakaba & Neher, 2001). However, synaptic transmission during AP trains is mainly carried by SVs of the fast-releasing, slowly-refilling pool (Sakaba, 2006; Neher, 2015). To investigate whether the observed effects in SV replenishment in calyces deficient in Bassoon or Piccolo are also reflected in RRP recovery in the absence of synaptic activity, we determined the recovery

induced by a RRP-depleting stimulus of 20 APs delivered at 100 Hz. RRP recovery was assessed by a test stimulus applied at various time intervals (0.01 s, 0.064 s, 0.128 s, 0.256 s, 0.512 s, 1.024 s, 2 s, 4 s, 6 s, 8 s, 10 s and 12 s) after the cessation of the AP train (Fig. 6A). The time course

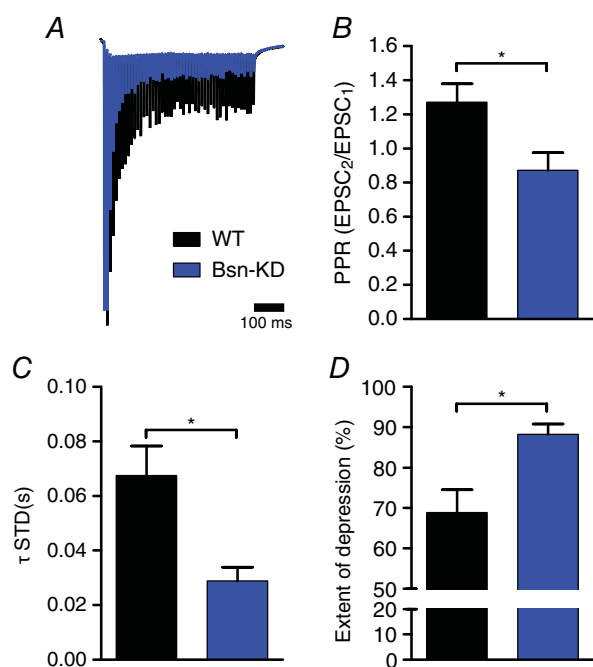


Figure 4. KD of Bassoon affects STD independent of P. A, superimposed scaled representative current traces recorded in response to 50 stimuli at 100 Hz in aCSF containing 1.5 mM extracellular calcium. B–D, quantification of the PPR, the time constant of EPSC amplitude decay and the extent of depression, respectively ($n = 9–6$). Error bars represent the SEM.

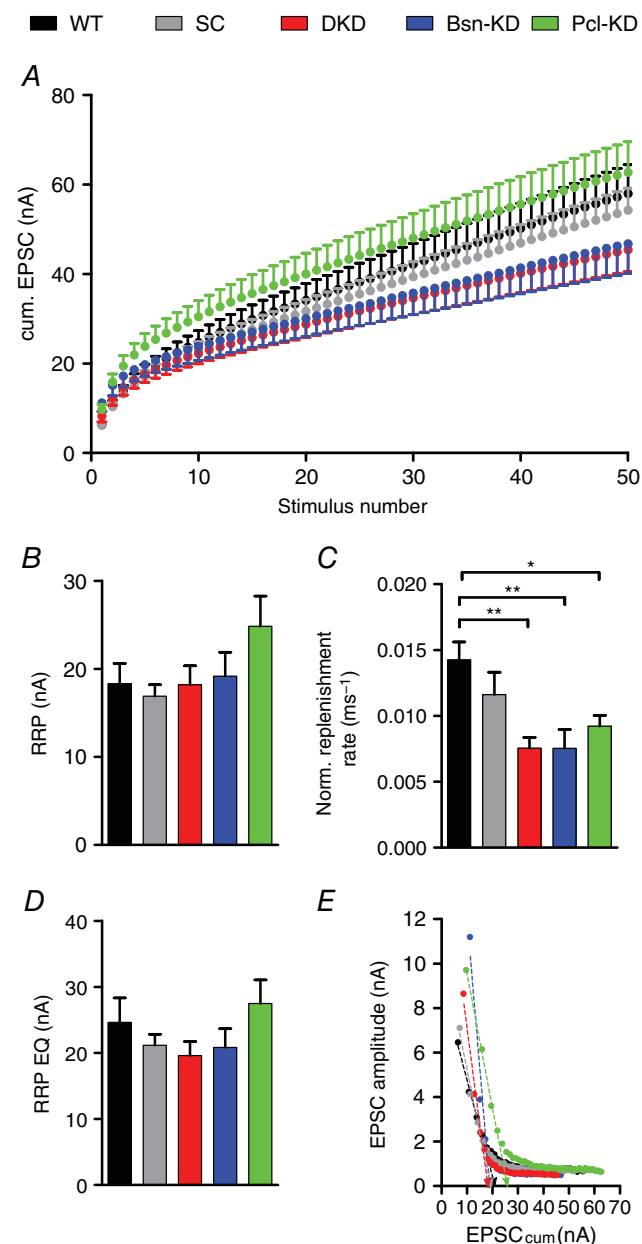


Figure 5. Bassoon and Piccolo regulate SV replenishment during ongoing stimulation

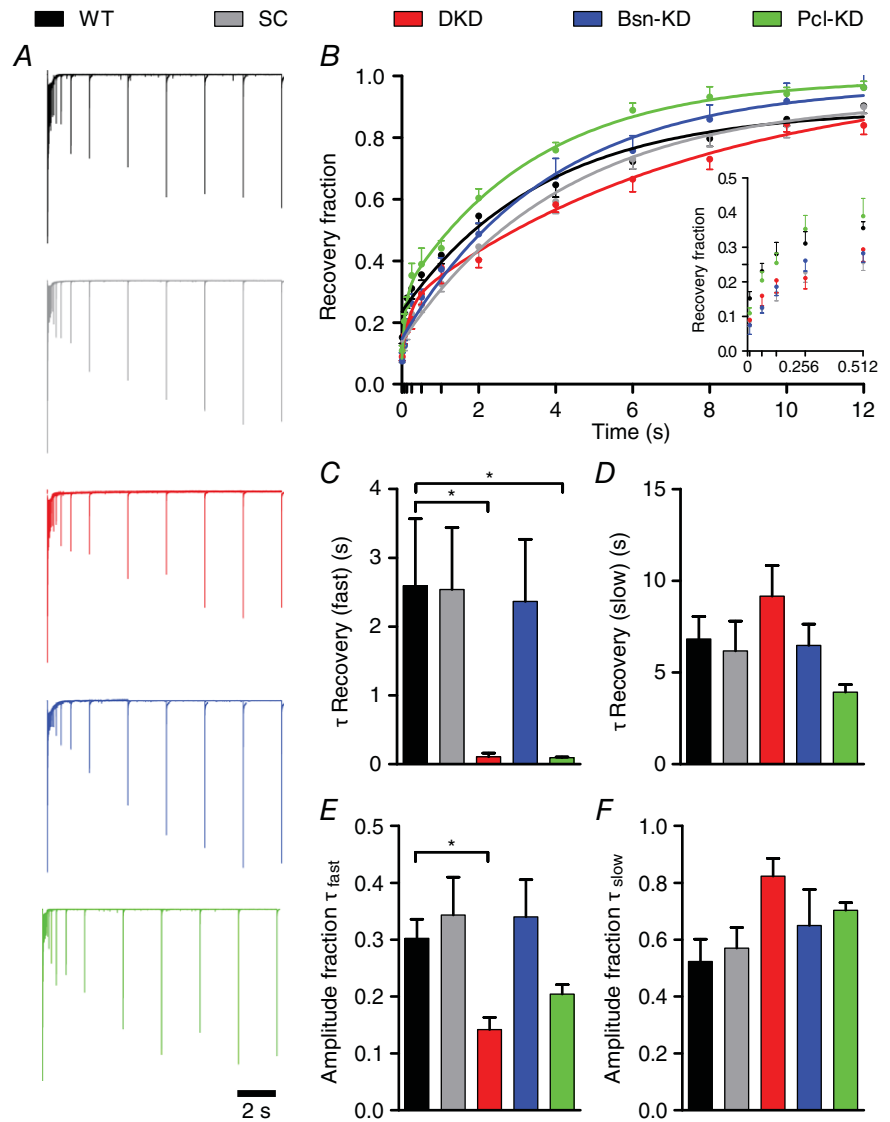
A, averaged cumulative EPSCs recorded during 100 Hz stimulus trains. B and C, quantification of RRP size and normalized SV replenishment rate (slope of the line fit divided by initial EPSC amplitude) ($n = 10–12$). D, quantification of RRP size as determined by the method described by Elmquist and Quastel ($n = 10–12$). E, representative plots of EPSC amplitudes vs. cumulative EPSC amplitudes obtained from single calyces. Error bars represent the SEM.

of recovery was well described by a mono-exponential function under our experimental conditions, probably reflecting primarily the refilling of the fast-releasing sub-pool. Surprisingly, the RRP recovery was best described by a bi-exponential function in calyces deficient in Piccolo (Pcl-KD and DKD) (Fig. 6A and B). To compare RRP recovery quantitatively, all recovery curves were fitted bi-exponentially. The slow time constant, representing the refilling of the fast-releasing SVs, was not changed by the expression of any of the shRNAs (Fig. 6D and Table 2). However, the fast time constant of recovery was significantly faster in Piccolo deficient calyces because their recovery was truly bi-exponential, whereas fitting of mono-exponential data (WT, SC and Bsn-KD) with a bi-exponential function results in ‘fast’ components with time constants similar to those of the slow ones (Fig. 6C and Table 2). This truly bi-exponential nature of the fits

describing the RRP recovery of DKD and Pcl-KD calyces was also reflected in the amplitude fractions of the two fit components (Fig. 6E and F and Table 2). The appearance of a fast component in the RRP recovery, and thus the release of slowly-releasing SVs during the AP trains in calyces lacking Piccolo but not Bassoon, suggests a unique function of Piccolo in the organization of the RRP.

Discussion

In the present study, we examined the roles of Bassoon and Piccolo during synaptic transmission at the calyx of Held by adapting a previously introduced shRNA-mediated KD approach (Leal-Ortiz *et al.* 2008; Waites *et al.* 2011, 2013; Okerlund *et al.* 2017) to *in vivo* conditions. Strong, specific KD of both proteins in individually identified terminals was found after expressing the shRNAs for 10 days. The



KD of Bassoon and Piccolo did not result in the loss of AZs in the present study, possibly because our *in vivo* approach typically does not reach the extent of KD achievable in cultured cells (Waites *et al.* 2013; Okerlund *et al.* 2017) (Fig. 1). Electrophysiological characterization of shRNA-expressing calyces revealed both shared and discrete functions of Bassoon and Piccolo. Both proteins control SV replenishment under ongoing activity, whereas only Piccolo organizes the AZ and the RRP to constrain the amount of SVs immediately released during AP trains. Hence, Piccolo may restrict the release of slowly-releasing SVs to periods of prolonged high-frequency activity, preventing synaptic transmission failures under such conditions.

Synaptic transmission: Bassoon

The effects of Bassoon deficiency have been examined at a variety of synapses with conflicting results. SV release has been found to be unaffected in the absence of Bassoon at cerebellar mossy fibre to granule cell synapses and in cultured hippocampal neurons after KD (Hallermann *et al.* 2010; Mukherjee *et al.* 2010), whereas other studies found reduced evoked release in hippocampal cultured neurons derived from Bassoon KO mice (Altrock *et al.* 2003) and increased spontaneous EPSC amplitudes at the endbulb of Held (Mendoza Schulz *et al.* 2014). The results obtained at the calyx of Held in the present study do not support a role for Bassoon in SV release (Fig. 2), although we cannot formally exclude it because the residual amount of Bassoon (~25%) might occlude potential effects. Bassoon interacts with a multitude of other presynaptic components, indicating an important function in organizing the AZ (Gundelfinger *et al.* 2016; Wang *et al.* 2009). Particularly, Bassoon has been suggested to selectively position P/Q-type VGCCs at SV release sites via its interaction with RIM-BP (Davydova *et al.* 2014). This implies that Bassoon-KD should affect the kinetics of evoked SV release as a result of altered coupling distances between SVs and VGCCs (Taschenberger & von Gersdorff, 2000; Fedchyshyn & Wang, 2005). EPSC kinetics were unchanged under our experimental conditions (postnatal day 12/13). However, the continued presence of N-type VGCCs at this age (Iwasaki & Takahashi, 1998) might have prevented us from detecting changes in EPSC kinetics because the positioning of N-type VGCCs is not affected by Bassoon (Davydova *et al.* 2014). Bassoon has been shown to slow down STD at synapses operating at high frequency by speeding up SV replenishment under ongoing synaptic activity (Hallermann *et al.* 2010; Mendoza Schulz *et al.* 2014), which is in line with the results obtained in the present study at the calyx of Held (Figs 3 and 5). Interestingly, although Piccolo KD has a clear effect on the SV replenishment rate and the relative extent of STD, the DKD phenocopies the KD of Bassoon only, with little

additive effects of Piccolo KD. This suggests that Bassoon is the dominant regulator of SV replenishment, a role that is further supported by the more prominent effects of Bassoon deficiency on STD compared to Pcl-KD synapses. Moreover, the effect of Bassoon on STD could be even more pronounced *in vivo* because both the time course of STD and the extent of depression are greatly affected by temperature (Kushmerick *et al.* 2006). Of note, we were unable to detect changes in the recovery from STD in Bsn-KD synapses, which have been reported previously (Hallermann *et al.* 2010; Mendoza Schulz *et al.* 2014). This may be a result of synapse-specific differences because the recovery from STD always follows a bi-exponential time course in the cerebellar mossy fibre terminals and endbulb of Held synapses used in earlier studies (Hallermann *et al.* 2010; Mendoza Schulz *et al.* 2014). Bassoon deficiency in these synapses selectively affects the fast component of recovery, which we do not consistently detect in our experimental system. However, our results agree with the previously published data because the mono-exponential recovery function used in the present study resembles the slow, unaffected component of the bi-exponential time course described at these two other synapses. Despite these insights into the functional role of Bassoon during high-frequency synaptic transmission at the calyx of Held, the underlying molecular mechanism(s) remain elusive and will be subject to future studies. Nevertheless, it is tempting to speculate that Bassoon may attract SVs to release sites via mechanisms involving RIM-BP, RIM and Rab3 (Gundelfinger *et al.* 2016; Davydova *et al.* 2014) or the SV docking protein Munc13, which has been shown to be involved in SV replenishment at the calyx (Lipstein *et al.* 2013) and also to interact with Piccolo (Gundelfinger *et al.* 2016).

Synaptic transmission: Piccolo

The role of Piccolo in synaptic transmission has received far less attention than that of Bassoon and has remained elusive because the existing studies report conflicting results: KD of Piccolo in hippocampal cultured neurons increased SV mobility and exocytosis (Leal-Ortiz *et al.* 2008; Waites *et al.* 2011), whereas the same type of neurons derived from Piccolo KO mice showed no changes in SV release (Mukherjee *et al.* 2010). KO of Piccolo in the endbulb of Held synapse resulted in slower SV replenishment, delayed recovery from STD and a reduced EPSC amplitude (Butola *et al.* 2017). Although we did not observe changes in SV release (e.g. EPSC amplitude) in Piccolo-deficient calyces, we found Piccolo to play a prominent role in SV replenishment during synaptic activity that may be mediated by Piccolo's interaction with Munc13 (Gundelfinger *et al.* 2016; Wang *et al.* 2009). Moreover, surprisingly, we found the time course of recovery from STD to change from mono- to bi-exponential in

calyces devoid of Piccolo (Fig. 6). Bi-exponential recovery from STD has been attributed to the release of two distinct SV populations within the RRP, fast-releasing but slowly-recovering SVs and slowly-releasing SVs that are refilled quickly (Wu & Borst, 1999; Sakaba & Neher, 2001). The appearance of a second, fast kinetic component during recovery from a RRP-depleting stimulus thus suggests that, in the absence of Piccolo, a fraction of the slowly-releasing subpool of the RRP becomes amenable to AP-induced release, whereas, in the presence of Piccolo, this pool is not available (Sakaba, 2006). Accordingly, Piccolo appears to restrict AP-induced SV release to the fast-releasing SV subpool at the calyx of Held, thereby establishing a subpool of SVs within the RRP that becomes available for release only during extended periods of intense activity and thus preventing synaptic transmission failures. The role of Piccolo in the maintenance of the slowly-releasing pool could even be more prominent under physiological conditions compared to those observed in the present study because the recovery from depression also depends on the temperature and frequency of the depleting stimulus (Kushmerick *et al.* 2006; Wang & Kaczmarek, 1998). The calyx of Held may rely heavily on the slowly-releasing vesicles retained by Piccolo during episodes of sound perception, when the synaptic activity at the calyx reaches frequencies of ~ 300 (Kopp-Scheinflug *et al.* 2008), to ensure faithful signal transmission. The molecular details of this function are presently unknown. They may include the organization of calcium buffers at the AZ to limit the spread of the AP-induced calcium transient from the VGCC towards the docked SVs. This would ensure that only SVs in close proximity of the VGCC sense a high enough calcium concentration to be released. Notably, Piccolo deficiency did not result in the recruitment of all slowly-releasing SVs because the fast recovering component accounted for only $\sim 15\%$ of total recovery (Fig. 6E and Table 2) instead of the $\sim 50\%$ reported previously at the calyx of Held (Wu & Borst, 1999; Sakaba & Neher, 2001). Moreover, Piccolo itself possesses two C_2 -domains in its C-terminal domain of which the C_2A domain binds calcium with low affinity and may thus act as a calcium sensor limiting SV availability to the fast RRP subpool (Gerber *et al.* 2001; Garcia *et al.* 2004). Alternatively, Piccolo function could depend on its interaction with actin-associated proteins such as Daam1 and Profilin2, thereby interfering indirectly with the dynamic regulation of F-actin during synaptic activity (Gundelfinger *et al.* 2016; Waites *et al.* 2011; Wagh *et al.* 2015). F-actin dynamics have been shown to play a role in RRP recovery at the calyx of Held (Sakaba & Neher, 2003; Lee *et al.* 2012). Moreover, actin has recently been shown to be crucial for ultrafast SV endocytosis (Watanabe *et al.* 2014; Delvendahl *et al.* 2016). Piccolo could therefore also regulate RRP recovery by affecting the rate of SV endocytosis via its interaction with

actin-associated proteins. However, the precise identity of the molecular mechanism(s) of Piccolo function will be subject to future studies.

Conclusions

The present study established both overlapping and distinct functions of Bassoon and Piccolo at the calyx of Held. A shared function of both proteins is the regulation of SV replenishment during ongoing activity at the AZ. Piccolo, however, uniquely restricts the AP-induced SV release to the fast-releasing fraction of the RRP, presumably consisting of SVs in the vicinity of the VGCCs. Taken together, we thus provide new insights into the enigmatic shared and unique functions of Bassoon and Piccolo during synaptic transmission at a central high-frequency-operating synapse. Moreover, the data reported in the present study may serve as a starting point for future studies on the molecular mechanisms underlying the functions of Bassoon and Piccolo.

References

- Altrock WD, tom Dieck S, Sokolov M, Meyer AC, Sigler A, Brakebusch C, Fässler R, Richter K, Boeckers TM, Potschka H, Brandt C, Löscher W, Grimberg D, Dresbach T, Hempelmann A, Hassan H, Balschun D, Frey JU, Brandstätter JH, Garner CC, Rosenmund C & Gundelfinger ED (2003). Functional inactivation of a fraction of excitatory synapses in mice deficient for the active zone protein bassoon. *Neuron* **37**, 787–800.
- Borst JG & Soria van Hoeve J (2012). The calyx of held synapse: from model synapse to auditory relay. *Annu Rev Physiol* **74**, 199–224.
- Butola T, Wichmann C & Moser T (2017). Piccolo promotes vesicle replenishment at a fast central auditory synapse. *Front Synaptic Neurosci* **9**, 14.
- Davydova D, Marini C, King C, Klueva J, Bischof F, Romorini S, Montenegro-Venegas C, Heine M, Schneider R, Schröder MS, Altrock WD, Henneberger C, Rusakov DA, Gundelfinger ED & Fejtova A (2014). Bassoon specifically controls presynaptic P/Q-type Ca(2+) channels via RIM-binding protein. *Neuron* **82**, 181–194.
- Delvendahl I, Vyleta NP, von Gersdorff H & Hallermann S (2016). Fast, temperature-sensitive and clathrin-independent endocytosis at central synapses. *Neuron* **90**, 492–498.
- Dondzillo A, Sätzler K, Horstmann H, Altrock WD, Gundelfinger ED & Kuner T (2010). Targeted three-dimensional immunohistochemistry reveals localization of presynaptic proteins Bassoon and Piccolo in the rat calyx of Held before and after the onset of hearing. *J Comp Neurol* **518**, 1008–1029.
- Elmqvist D & Quastel DM (1965). A quantitative study of end-plate potentials in isolated human muscle. *J Physiol* **178**, 505–529.

- Fedchyshyn MJ & Wang LY (2005). Developmental transformation of the release modality at the calyx of Held synapse. *J Neurosci* **25**, 4131–4140.
- Frank T, Rutherford MA, Strenzke N, Neef A, Pangršič T, Khimich D, Fetjova A, Gundelfinger ED, Liberman MC, Harke B, Bryan KE, Lee A, Egnér A, Riedel D & Moser T (2010). Bassoon and the synaptic ribbon organize Ca²⁺ channels and vesicles to add release sites and promote refilling. *Neuron* **68**, 724–738.
- García J, Gerber SH, Sugita S, Südhof TC & Rizo J (2004). A conformational switch in the Piccolo C2A domain regulated by alternative splicing. *Nat Struct Mol Biol* **11**, 45–53.
- Gerber SH, García J, Rizo J & Südhof TC (2001). An unusual C(2)-domain in the active-zone protein piccolo: implications for Ca(2+) regulation of neurotransmitter release. *EMBO J* **20**, 1605–1619.
- Grundy D (2015). Principles and standards for reporting animal experiments in The Journal of Physiology and Experimental Physiology. *J Physiol* **593**, 2547–2549.
- Gundelfinger ED & Fetjova A (2012). Molecular organization and plasticity of the cytomatrix at the active zone. *Curr Opin Neurobiol* **22**, 423–430.
- Gundelfinger ED, Reissner C & Garner CC (2016). Role of Bassoon and Piccolo in assembly and molecular organization of the active zone. *Front Synaptic Neurosci* **7**, 19.
- Hallermann S, Fetjova A, Schmidt H, Weyhersmüller A, Silver RA, Gundelfinger ED & Eilers J (2010). Bassoon speeds vesicle reloading at a central excitatory synapse. *Neuron* **68**, 710–723.
- Ivanova D, Dirks A, Montenegro-Venegas C, Schöne C, Altmann WD, Marini C, Frischknecht R, Schanze D, Zenker M, Gundelfinger ED & Fetjova A (2015). Synaptic activity controls localization and function of CtBP1 via binding to Bassoon and Piccolo. *EMBO J* **34**, 1056–1077.
- Iwasaki S & Takahashi T (1998). Developmental changes in calcium channel types mediating synaptic transmission in rat auditory brainstem. *J Physiol* **509**, 419–423.
- Jing Z, Rutherford MA, Takago H, Frank T, Fetjova A, Khimich D, Moser T & Strenzke N (2013). Disruption of the presynaptic cytomatrix protein bassoon degrades ribbon anchorage, multiquantal release, and sound encoding at the hair cell afferent synapse. *J Neurosci* **33**, 4456–4467.
- Kaaser PS & Regehr WG (2014). Molecular mechanisms for synchronous, asynchronous, and spontaneous neurotransmitter release. *Annu Rev Physiol* **76**, 333–363.
- Khimich D, Nouvian R, Pujol R, tom Dieck S, Egnér A, Gundelfinger ED & Moser T (2005). Hair cell synaptic ribbons are essential for synchronous auditory signalling. *Nature* **434**, 889–894.
- Kopp-Scheinplugg C, Tolnai S, Malmierca MS & Rübsamen R (2008). The medial nucleus of the trapezoid body: comparative physiology. *Neuroscience* **154**, 160–170.
- Körber C, Horstmann H, Venkataramani V, Herrmannsdörfer F, Kremer T, Kaiser M, Schwenger DB, Ahmed S, Dean C, Dresbach T & Künér T (2015). Modulation of presynaptic release probability by the vertebrate-specific protein mover. *Neuron* **87**, 521–533.
- Körber C & Künér T (2016). Molecular machines regulating the release probability of synaptic vesicles at the active zone. *Front Synaptic Neurosci* **8**, 5.
- Kushmerick C, Renden R & von Gersdorff H (2006). Physiological temperatures reduce the rate of vesicle pool depletion and short-term depression via an acceleration of vesicle recruitment. *J Neurosci* **26**, 1366–1377.
- Leal-Ortiz S, Waites CL, Terry-Lorenzo R, Zamorano P, Gundelfinger ED & Garner CC (2008). Piccolo modulation of synapsin1a dynamics regulates synaptic vesicle exocytosis. *J Cell Biol* **181**, 831–846.
- Lee JS, Ho WK & Lee SH (2012). Actin-dependent rapid recruitment of reluctant synaptic vesicles into a fast-releasing vesicle pool. *Proc Natl Acad Sci USA* **109**, E765–774.
- Lipstein N, Sakaba T, Cooper BH, Lin KH, Strenzke N, Ashery U, Rhee JS, Taschenberger H, Neher E & Brose N (2013). Dynamic control of synaptic vesicle replenishment and short-term plasticity by Ca(2+)-calmodulin-munc13-1 signaling. *Neuron* **79**, 82–96.
- Mendoza Schulz A, Jing Z, Sánchez Caro JM, Wetzel F, Dresbach T, Strenzke N, Wichmann C & Moser T (2014). Bassoon-disruption slows vesicle replenishment and induces homeostatic plasticity at a CNS synapse. *EMBO J* **33**, 512–527.
- Mukherjee K, Yang X, Gerber SH, Kwon HB, Ho A, Castillo PE, Liu X & Südhof TC (2010). Piccolo and bassoon maintain synaptic vesicle clustering without directly participating in vesicle exocytosis. *Proc Natl Acad Sci USA* **107**, 6504–6509.
- Neher E (2015). Merits and limitations of vesicle pool models in view of heterogeneous populations of synaptic vesicles. *Neuron* **87**, 1131–1142.
- Okerlund ND, Schneider K, Leal-Ortiz S, Montenegro-Venegas C, Kim SA, Garner LC, Gundelfinger ED, Reimer RJ & Garner CC (2017). Bassoon controls presynaptic autophagy through Atg5. *Neuron* **93**, 897–913.
- Rizzoli SO (2014). Synaptic vesicle recycling: steps and principles. *EMBO J* **33**, 788–822.
- Sakaba T (2006). Roles of the fast-releasing and the slowly releasing vesicles in synaptic transmission at the calyx of Held. *J Neurosci* **26**, 5863–5871.
- Sakaba T & Neher E (2001). Calmodulin mediates rapid recruitment of fast-releasing synaptic vesicles at a calyx-type synapse. *Neuron* **32**, 1119–1131.
- Sakaba T & Neher E (2003). Involvement of actin polymerization in vesicle recruitment at the calyx of Held synapse. *J Neurosci* **23**, 837–846.
- Schneggenburger R, Meyer AC & Neher E (1999). Released fraction and total size of a pool of immediately available transmitter quanta at a calyx synapse. *Neuron* **23**, 399–409.
- Schwenger DB & Künér T (2010). Acute genetic perturbation of exocyst function in the rat calyx of Held impedes structural maturation, but spares synaptic transmission. *Eur J Neurosci* **32**, 974–984.
- Südhof TC (2012). The presynaptic active zone. *Neuron* **75**, 11–25.
- Taschenberger H, Leão RM, Rowland KC, Spirou GA & von Gersdorff H (2002). Optimizing synaptic architecture and efficiency for high-frequency transmission. *Neuron* **36**, 1127–1143.

- Taschenberger H & von Gersdorff H (2000). Fine-tuning an auditory synapse for speed and fidelity: developmental changes in presynaptic waveform, EPSC kinetics, and synaptic plasticity. *J Neurosci* **20**, 9162–9173.
- Traynelis SF, Wollmuth LP, McBain CJ, Menniti FS, Vance KM, Ogden KK, Hansen KB, Yuan H, Myers SJ & Dingledine R (2010). Glutamate receptor ion channels: structure, regulation, and function. *Pharmacol Rev* **62**, 405–496.
- Wagh D, Terry-Lorenzo R, Waites CL, Leal-Ortiz SA, Maas C, Reimer RJ & Garner CC (2015). Piccolo directs activity dependent F-actin assembly from presynaptic active zones via Daam1. *PLoS ONE* **10**, e0120093.
- Waites CL, Leal-Ortiz SA, Andlauer TF, Sigrist SJ & Garner CC (2011). Piccolo regulates the dynamic assembly of presynaptic F-actin. *J Neurosci* **31**, 14250–14263.
- Waites CL, Leal-Ortiz SA, Okerlund N, Dalke H, Fejtova A, Altmann WD, Gundelfinger ED & Garner CC (2013). Bassoon and Piccolo maintain synapse integrity by regulating protein ubiquitination and degradation. *EMBO J* **32**, 954–969.
- Wang LY & Kaczmarek LK (1998). High-frequency firing helps replenish the readily releasable pool of synaptic vesicles. *Nature* **394**, 384–388.
- Wang X, Hu B, Zieba A, Neumann NG, Kasper-Sonnenberg M, Honsbein A, Hultqvist G, Conze T, Witt W, Limbach C, Geitmann M, Danielson H, Kolarow R, Niemann G, Lessmann V & Kilimann MW (2009). A protein interaction node at the neurotransmitter release site: domains of Aczonin/Piccolo, Bassoon, CAST, and rim converge on the N-terminal domain of Munc13-1. *J Neurosci* **29**, 12584–12596.
- Watanabe S, Trimbuch T, Camacho-Pérez M, Rost BR, Brokowski B, Söhl-Kielczynski B, Felies A, Davis MW, Rosenmund C & Jorgensen EM (2014). Clathrin regenerates synaptic vesicles from endosomes. *Nature* **515**, 228–233.
- Wimmer VC, Nevian T & Kuner T (2004). Targeted in vivo expression of proteins in the calyx of Held. *Pflügers Archiv* **449**, 319–333.
- Wu LG & Borst JG (1999). The reduced release probability of releasable vesicles during recovery from short-term synaptic depression. *Neuron* **23**, 821–832.
- Zucker RS & Regehr WG (2002). Short-term synaptic plasticity. *Annu Rev Physiol* **64**, 355–405.

Additional information

Competing interests

The authors declare that they have no competing financial interests.

Author contributions

CK and TK designed the experiments. DP and CK acquired and analysed the data. CK drafted the manuscript with contributions from all the other authors. All authors approved the final version submitted for publication and agree to be accountable for all aspects of the work in ensuring that questions related to the accuracy and integrity of any part of the work are appropriately investigated and resolved. All persons designated as authors qualify for authorship, and all those who qualify are listed.

Funding

This study was supported by the Deutsche Forschungsgemeinschaft (DFG) via the Collaborative Research Centre 1134 (to TK and CK) and the Priority Program 1608 (to CK).

Acknowledgements

The authors are grateful to Michaela Kaiser, Claudia Kocksch and Marion Schmitt for excellent technical assistance.